VOL. 12, NO. 10, MAY 2017 ISSN 1819-6608
ARPN Journal of Engineering and Applied Sciences
©2006-2017 Asian Research Publishing Network (ARPN). All rights reserved.

www.arpnjournals.com

NUMERICAL SIMULATION OF PCM INTERGRATED SOLAR COLLECTOR STORAGE WATER HEATER

Muhammad Redzuan, C. N[1]., Saw, C. L. [1], Lew, W. C.[2], Choong, C. G.[1], Salvinder, S.[3], H. H. Al-Kayiem[4] and Afolabi Lukmon[4]
[1]Center of Air Conditioning and Refrigeration, Politeknik Ungku Omar, Ipoh, Perak, Malaysia
[2]Department of Electrical Engineering, Politeknik Ungku Omar, Ipoh, Perak, Malaysia
[3]Center of Marine Engineering, Politeknik Ungku Omar, Ipoh, Perak, Malaysia
[4]Department of Mechanical Engineering, Universiti Teknologi Petronas, Ipoh, Perak, Malaysia
E-Mail: mredzuannoordin@puo.edu.my

ABSTRACT

Solar water heater has been widely used in domestic and industrial sectors to harvest the available solar radiation daily to produce hot water. Computational analysis on performance of solar water heater has been trending up to offset the higher cost of experimental measurement. A 3D computational fluids dynamics (CFD) model was developed and validate with experimental results. The average hot water temperature simulated at 1.00PM until 5.00PM variesfrom 49.0 ºC to 54.9 ºC, while average PCM temperature varies from 53.0 ºC to 64.8 ºC. The CFD models developed shows a good agreement of 6.7% and 7.1% simulation error for hot water temperature and PCM temperature respectively. The simulation model developed can be used as a prediction tool for solar energy research and to reduce cost on development of experimental test rig for solar collector experiment.

Keywords: PCM, solar integrated collector, 3D CFD model, solar load model's ray tracing algorithm, solidification & melting model.

INTRODUCTION

A solar integrated collector water heating is a combination of collector and storage in a single unit. The collector storage is used to fill up phase change material (PCM) such as paraffin wax, hydrate salt or PCM nanocomposite. Solar collector particularly is a heat exchanger that convert solar radiation in heat at low, medium and high temperature at day time. While, in the night time, PCM transferred heat to solar collector to heat up hot water or hot air. The low temperature solar integrated collector are used in many application such as water heating, local space heating and solar drying of agriculture and marine products that need heat temperature of 30 ºC to 90 ºC[1-2].

Numbers of study on performance of solar water heater based on phase-changing material was carried out due to the effectiveness of latent heat PCM [3-4]. The improvement on the computer has encourage the used to computational simulation to analyze the performance of solar collector and solar integrated collector. There are few approaches for the computational simulation that is computational fluid dynamic (CFD), artificial neural-networks (ANN), transient simulation tool (TRNSYS) and finite element analysis (FEA) mainly used by researchers [5-7]. Simulation of 1D and 2D CFD model have been widely investigated but 3D CFD simulation is complicated and required high speed computer. Not many study on 3D CFD simulation of solar integrated water heater system especially integrated with PCM. There are studies on solar integrated collector but the storage is water for heating purposes [8-9]. In the paper, a 3D CFD model was developed with dimension 1m x 1m and simulated using melting and solidification Model, Viscous Model and Radiation Model. SIMPLEC Scheme is used as discretization method for the simulation. The simulation results are used to validate with the experimental result measured by Al-Kayiem (2014) [10].

NUMERICAL SOLUTION

The numerical modeling and analysis og the solar integrated collector storage system has been carried out using the commercial CFD software ANSYS FLUENT version 15. The geometry was modeled in Autodesk Inventor 2014 then imported to ANSYS FLUENT for mesh generation. An enthalphy porosity technique is used in FLUENT for modeling the solidification/melting process. In this technique, the melt interface was not tracked explicitly. Instead, a quantity called the liquid fraction, which indicates the fraction of the cell in the domain. Some assumptions were made in the numerical calculations: the heat conductivity and density of the phase-change material and the enclosures are constant; the values for the PCM were chosen as average of the solid and liquid material properties. The problem was solved in Three-dimensional domain. The heat transfer in the z direction and the convection heat transfer coefficient in the liquid PCM during the solidification process have been neglected.

Governing equations for melting and solidification model

The governing equations for transient analysis of melting of the phase-change material include the the Navier-Stokes (momentum) equations, the continuity equation and the energy equation. Boussinesq approximation is used to model the bouyancy forces. The equations are given in tensor notation for solidification and melting model as mentioned by Reddy (2007) [11]:

©2006-2017 Asian Research Publishing Network (ARPN). All rights reserved.

Continuity equation:

$$\nabla \cdot \vec{v}=0 \quad (1)$$

Momentum equation :

$$\rho \frac{\delta \vec{v}}{\delta t}+\rho(\vec{v}.\nabla)\vec{v}=-\nabla\rho + \mu\nabla^2\vec{v}+\rho\vec{g}\beta(T - T_o) \quad (2)$$

Energy equation:

$$\rho c_\rho(\frac{\delta T}{\delta t} + \vec{v}.\nabla T)=\nabla(K\nabla T) \quad (3)$$

For the solid PCM and the enclosure, the continuity and momentum equations can be ignored because there is no convection effect on the materials. The energy equation is given as

$$p_s cp_s(\frac{\delta T_S}{dt})=\nabla(k_s \nabla T_S) \quad (4)$$

The subscript *s* denotes the solid PCM or the enclosure. The energy balance for the solid-liquid interface in the melting process is expresses as

$$k_s \frac{dT_s}{dn}|s - k_l \frac{dT_s}{dn}|s=p_s L \frac{dS_n}{dt} \quad (5)$$

Where *S* is the solid-liquid phase-change interface; *n* is the normal of the solid-liquid interface and L the latent heat of PCM fusion. In the solidification process, the subscripts *l* and *s* are interchanged and the latent heat of fusion L is replaced with-L in Equation. (5).

SIMULATION MODEL and SIMULATION SETUP

Figure-1 and Figure-2 show the isometry view of solar water heater with dimension of 1m x1m and the components included for solar integrated solar water heating system.

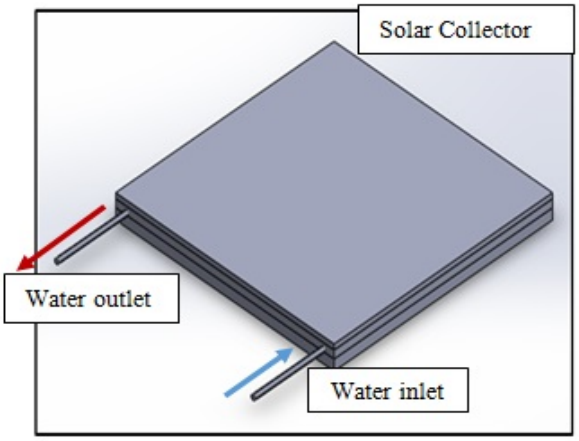

Figure-1. Isometry view of solar water heater.

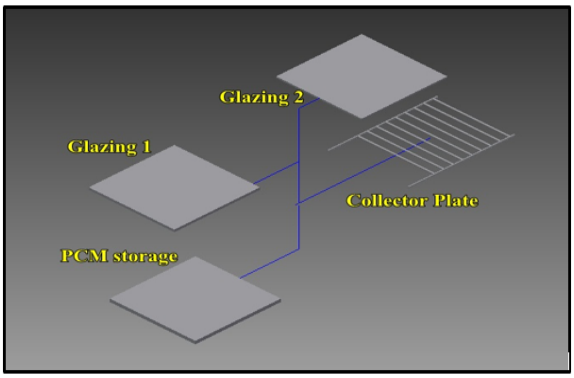

Figure-2. Isometry view of solar water heater.

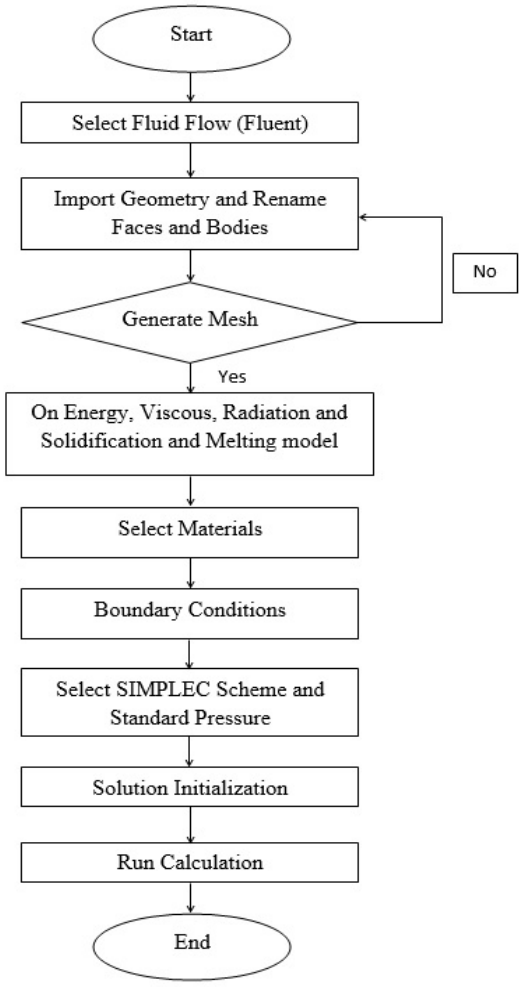

Figure-3. Boundary condition and simulation setup.

On the simulation process, Energy model, Turbulent model (k-epsilon), Solar Load model's Ray Tracing Algorithm and Solidification & Melting model have been selected as shown in Figure-3. Solar Load model's Ray Tracing Algorithm is used since there is solar radiation data captured during experimental measurement as an input value. Latitude of 101.48º, Longitude of 4.68º,

©2006-2017 Asian Research Publishing Network (ARPN). All rights reserved.

flow rate of 0.5 L/min and average solar radiation data at 1.00PM till 5.00PM are filled in the ANSYS FLUENT. Water flow at 0.5 L/min all the time to collect heat from solar collector to water storage tank for heat storing. The input data of solar radiation heat flux (W/m^2) are the average of 3 days measurement data hourly. Time step of 3600 seconds is used to simulate each hour. 18000s have been used for simulation 12.00 PM – 5PM. The 3D model has been simulated at 1.00 PM to 5 PM with meshing of 305000 mesh cell by SIMPLEC scheme. Time 1.00PM till 5.00PM is choosen due to best available solar radiation daily.

Material properties

While, the properties used in the simulation as listed in Table-1, while the dimension of the components in the simulation model are the same as real prototype are listed in Table-2.

Table-1. Properties of material [12].

Parameter	Glazing 1	Glazing 2	Absorber Plate
Materials	Glass	Glass	Copper
Density (kg/m^3)	750	750	8978
Thermal Conductivity (W/mK)	0.5	387.6	0.0242
Viscosity (kg/ms)	-	-	-
Thermal Expansion (1/°C)	-	-	-
Solidus temperature (°C)	-	-	-
Liqidus temperature (°C)	-	-	-
Materials	Paraffin Wax	Wood	
Density (kg/m^3)	804.3	700	
Thermal Conductivity (W/mK)	2412	2130	
Viscosity (kg/ms)	6.3x10^{-3}	-	
Thermal Expansion (1/°C)	7.14x10^{-3}	-	
Solidus temperature (°C)	46	-	
Liqidus temperature (°C)	48	-	

Table-2. Dimension of the real prototype.

Components	Dimensions	Dimensions (cm)
PCM Storage	Width	100
	Length	100
	Thickness	2
Pipe Collector	Width	88
	Length	115
	Diameter	1
Glazing	Width	100
	Length	100
	Thickness glazing 1	1.5
	Thickness glazing 2	1

RESULTS AND DISCUSSIONS

Figure-4 shows the average hot water produced simulated varies from 49.0 °C to 54.9 °C at 1.00PM until 5.00PM. Figure-5 shows the average simulated PCM temperature varies from 53.0 °C to 64.8 °C. This is also shows that when the solar radiation reduces the radiation captured then converted to heat also reduces, hence reduced the temperature of heating water and PCM.

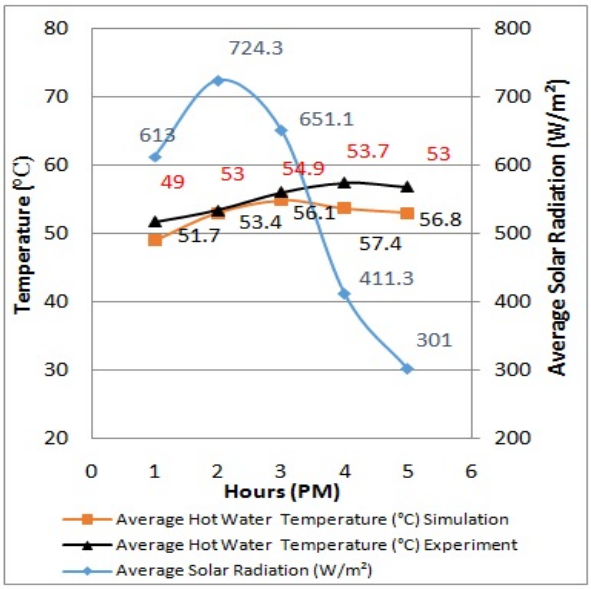

Figure-4. Variation of average solar radiation, simulated average hot water temperature and experimental average hot water temperature.

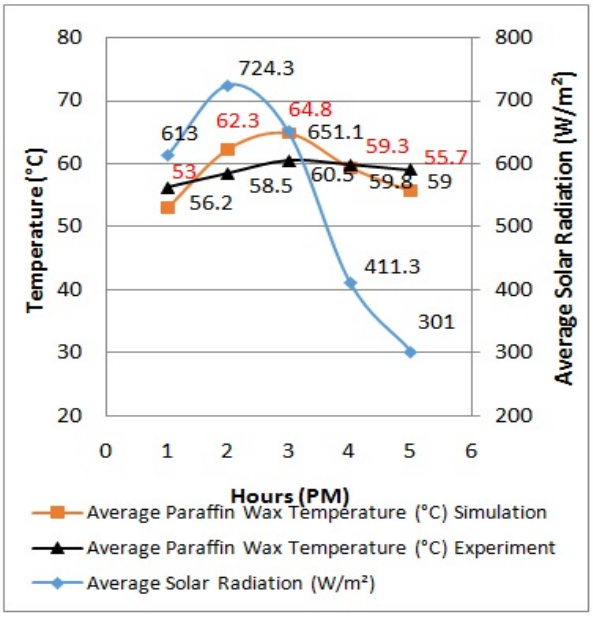

Figure-5. Variation of average solar radiation, simulated average PCM temperature and experimental average PCM temperature.

©2006-2017 Asian Research Publishing Network (ARPN). All rights reserved.

Table-3. Simulated average water and PCM temperature at 1.00 PM to 5.00PM.

Parameter	1.00PM	2.00PM	3.00PM
Average solar radiation (W/m^2)	613.0	724.3	651.1
Hot water temperature Experiment (°C)	51.7	53.4	56.1
Hot water temperature Simulation (°C)	49.0	53.0	54.9
Temperature difference (°C)	2.7	0.4	1.2
Percentage error (%)	5.2	0.7	2.1
Average temperature of PCM	53.0	62.3	64.8
Average temperature of PCM (Experiment)	56.2	58.5	60.5
Percentage error (%)	5.6	6.5	7.1
Parameter	**4.00PM**	**5.00PM**	
Average solar radiation (W/m^2)	411.3	301.0	
Hot water temperature Experiment (°C)	57.4	56.8	
Hot water temperature Simulation (°C)	53.7	53.0	
Temperature difference (°C)	3.7	3.8	
Percentage error (%)	6.4	6.7	
Average temperature of PCM	59.3	55.7	
Average temperature of PCM (Experiment)	59.8	59.0	
Percentage error (%)	0.8	5.6	

Table-4 shows the temperature contours of solar collector at 1.00 PM, the average hot water temperature is 49.0 °C while at 2.00 PM is 53.0 °C. The value of average hot water temperature with PCM at 3.00 PM is 54.3 °C. on the other hand, the average hot water at 4.00 PM is 54.9 °C and 5.00 PM is 53.0 °C. As from 12.00PM to 5.00PM, the value of temperature different is between 0.4 °C to 3.8 °C are showed in Table-5. The lowest value of temperature different and percentage error is at 2.00PM and 3.00PM. The average hot water temperature at 2.00PM is 53.4 °C based on experiment and 53.0 °C based on simulation because PCM (paraffin wax) that used has a good thermal conductivity to store heat. The experiment value and simulation slightly different in term of temperature error. It is due to the heat losses during heat transfer and conversion of heat solar radiation when through one part to other part. Good insulation is also crucial for reducing the heat loss from the solar collector to environment. These maximum simulation percentage error obtained is 6.7% and 7.1% for water temperature and PCM temperature respectively.

Table-4. Solar collector temperature contour Isometry view.

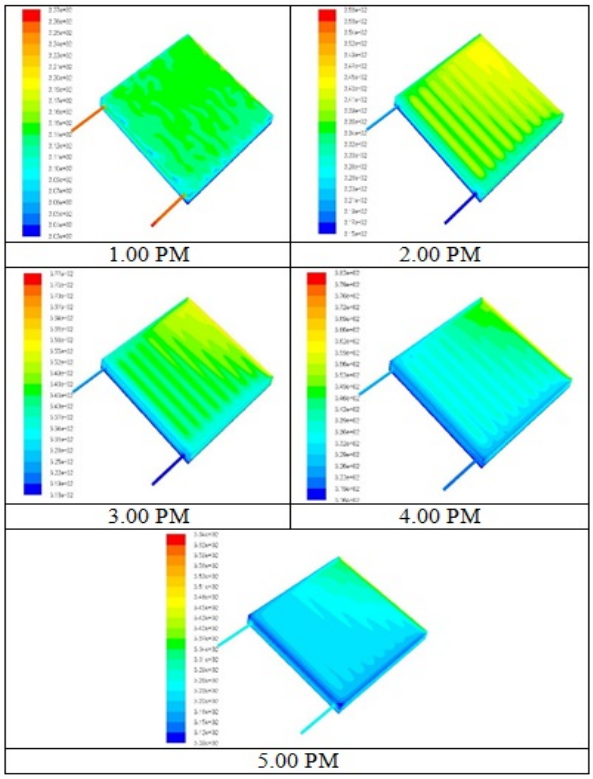

Table-5. Hot water temperature contour.

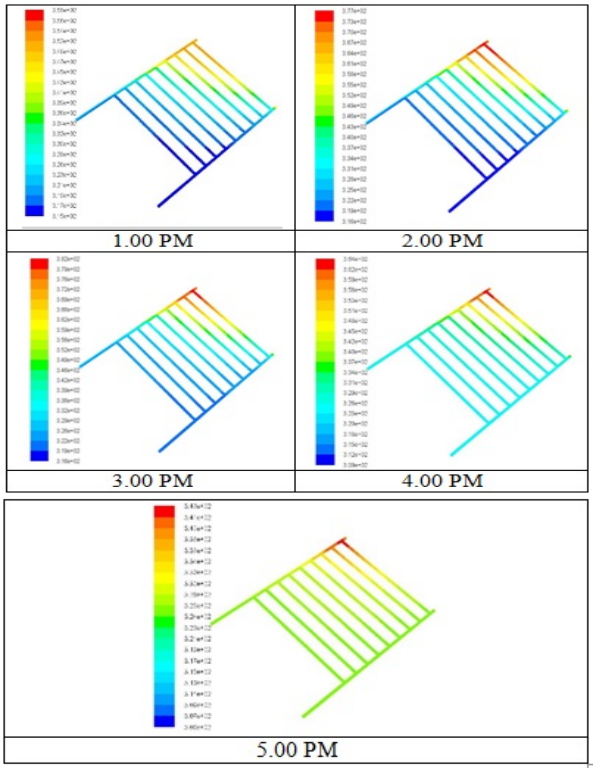

©2006-2017 Asian Research Publishing Network (ARPN). All rights reserved.


CONCLUSIONS

3D CFD models has been developed and validate with experimental measurement results. The percentage of error ±7.1% shows that the CFD model has a good agreement with the experimental results. Simulation on the water temperature shows a close agreement while, paraffin wax melting simulation are varies when compared with experimental results. Further simulation on the day time and night time is crucial to evaluate the validity of the 3D CFD models. Higher order of discretization scheme are suggested to improve the accuracy of the simulation.

REFERENCES

[1] A. Sharma, V.V. Tyagi, C.R. Chen, D. Buddhi.2009. Review on thermal energy storage with phase change materials and application. Renew. Sust. Energy Rev. 13: 318-345.

[2] H. H. Al-Kayiem,S. C. Lin, A. Lukmon. 2013. Review on nanomaterials for thermal energy storage technologies. J. Nanosci. Nanotechnol.-Asia. 3 (1).

[3] K. Ahmet,A. Ozmerzi and S. Bilgin. 2002. Thermal performance of a water-phase change material solar collector. Renewable Energy. 26(3): 391-399.

[4] C. Monia, M. Hatem and B. Philippe. 2014. Thermal performance of an integrated collector storage solar water heater (ICSSWH) with phase change materials (PCM). Energy Conversion and Management. (78): 897-903.

[5] S. Basavanna and KCFD. Shashishekar. 2013. Analysis of triangular absorber tube of a solar flat plate collector. Int J Mech Eng Robot Res. 1:19–24.

[6] D. Henderson, H. Junaidi, T. Muneer, T. Grassie, J. Currie. 2007. Experimental and CFD Investigation of an ICSSWH at various inclinations. Renew Sustain Energ Rev. 11:1087–116.

[7] A. Luca, Tagliafico, S. Federico, D. R. Mattia. 2014. Dynamic thermal models and CFD analysis for flat-plate thermal solar collector – A review. Renewable and Sustainable Energy Reviews. (30): 526-537.

[8] K. Gertzos, S. Pnevmatikakis and Caourisy. 2008. Experimental and numerical study of heat transfer phenomena, inside a flat-plate integrated collector storage solar water heater (ICSSWH), within direct heat withdrawal. Energy Convers Manage. 49:3104–15.

[9] K. Gertzos and Caourisy. 2008. Optimal arrangement of structural and functional parts in a flat plate integrated collector storage solar water heater (ICSSWH). Exp Therm Fluid Sci. 32: 1105–17.

[10] H. H. Al-Kayiem and S. C. Lin. 2014. Performance evaluation of a solar water heater integrated with a PCM nanocomposite TES at various inclinations. Sol. Energy.109: 82–92.

[11] K. S. Reddy. 2007. Thermal modelling of PCM based solar integrated collector storage water heating system. J. Sol. Energy Eng. 129 (4): 458-464.

[12] J. F. Marian and A. F. C. William. 1982. Introduction to solar technology, Addison–Wesley Publishing Company, Inc.pp. 68–70.